The Benefits of Resource Partitioning and Division of Labor in Microbial Consortia

Diana Schepens[1], Ashley E. Beck[2,4], Jeffrey J. Heys[3], Tomas Gedeon[1] and Ross P. Carlson[3,4]

[1] Department of Mathematical Sciences
[2] Department of Microbiology and Immunology
[3] Department of Chemical and Biological Engineering
[4] Center for Biofilm Engineering
Montana State University-Bozeman, Montana, 59717 USA

Abstract

Microbial communities composed of different species are frequently observed in nature. There is growing interest in understanding the advantages of living in a mixed species community as compared to a monoculture. Understanding the effects of microbial interactions will lead to better control of environmental microbial systems responsible for nutrient cycling, medical systems like the human GI tract or chronic wounds, and applied systems like biofuel synthesis. We examine two different advantages associated with interacting microbial communities operating as a food chain. The first advantage is the minimization of anabolic resource investment required to drive a constant flux through a series of enzyme-catalyzed reactions. The second advantage is enhanced productivity of a biofilm community when inhibitory byproducts are consumed by a scavenger population.

1 Introduction

Microorganisms acquire resources from their environment, which are processed via series of enzymes into cellular energy and biomass, and metabolic byproducts are secreted. Species that are efficient at deriving cellular energy and biomass from available resources, typically grow and reproduce faster than less efficient species [11]. This simplified view suggests communities should consist of a monoculture of the most 'efficient' species, sometimes termed 'superorganisms'. Superorganisms are not observed in nature. Instead, complex communities of interacting microorganisms are observed [6]. Potential advantages of mixed communities relative to monocultures include efficiency gains from specialization, the development of advanced functions, the ability to better tolerate environmental fluctuations, the utilization of inhibitory byproducts by other community members, and lower susceptibility to a single predatory attack, among many possible advantages.

The focus here is on food chains within microbial communities, specifically, systems where one population consumes metabolites excreted by others. These types of interactions are frequently referred to as syntrophic interactions [13]. Food chains are commonly observed in natural and applied systems including the cycling of carbon during the degradation of lignocellulosic material or the cycling of nitrogen in waste water treatment facilities [10]. Additionally, food chains have been observed to evolve repeatedly in the laboratory environment. For example, chemostats inoculated with a single *Escherichia coli* strain and operated under carbon-limited conditions will evolve spontaneously into a community of crossfeeding sub-strains. The evolved communities consist of one strain specializing in glucose catabolism and other strains specializing in catabolism of secreted inhibitory byproducts like acetate. The overall system demonstrates a 15% improvement in biomass production from the limiting resource glucose [9].

While there are many potential benefits for microorganisms existing in a mixed community, the focus here is on a theoretical analysis of two possible benefits associated with resource exchange: enhanced return on limiting anabolic resource and lowered byproduct inhibition. The first benefit is quantified by solving a constrained optimization model of a series of reactions controlled by resource investment into different substrate and enzyme pools, and the second benefit is reduced byproduct accumulation quantified using individual-based models of a biofilm community.

2 First Benefit: Enhanced Return on Anabolic Resource Investment

Cellular flux is driven by combinations of resource investments into both substrate and enzymes pools. Consider an n reaction enzymatic pathway

$$S_1 \overset{E_1}{\rightarrow} S_2 \overset{E_2}{\rightarrow} \cdots \overset{E_{n-1}}{\rightarrow} S_n \overset{E_n}{\rightarrow} P,$$

where the substrate S_1 is transformed into product P with the help of n enzymes, $E_1, ..., E_n$. In a limited resource environment, microorganisms that maximize the functional return on resource investment will be competitive [2]. To examine the trade-off between investment into combinations of substrate and enzyme pools, we assume that the cell can partition an essential resource (e.g. carbon) into optimal combinations of substrate pools utilized in this enzymatic pathway and into building the enzymes $E_1, ..., E_n$. Both substrate pools and enzymes represent resource investments but with different resource liquidity. If substrate S_i consists of b_i carbon atoms and enzyme E_i consists of a_i carbon atoms, then the total carbon investment for the enzymatic pathway

is:

$$C := \sum_{i=1}^{n}([E_i]a_i + [S_i]b_i).$$

Our model of the enzymatic pathway takes the form of a set of differential equations:

$$\dot{S}_1 = k_{a_1}S_0 - \frac{V_1[S_1]}{\kappa_1 + [S_1]},\ \dot{S}_2 = \frac{V_1[S_1]}{\kappa_1 + [S_1]} - \frac{V_2[S_2]}{\kappa_2 + [S_2]},\ \dot{P} = \frac{V_n[S_n]}{\kappa_n + [S_n]} - k_{a_2}[P],$$

where $k_{a_1}[S_0]$ is a constant source term and $[P]$ is the concentration of the final product. Here $V_i = [E_i]k_i$ and we assume a one-to-one stochiometric relationship between S_i and S_{i+1} as catalyzed by E_i. Assuming the pathway is at steady state we obtain

$$k_{a_1}S_0 = \frac{V_1[S_1]}{\kappa_1 + [S_1]} = \frac{V_2[S_2]}{\kappa_2 + [S_2]} = \ldots = \frac{V_n[S_n]}{\kappa_n + [S_n]} = k_{a_2}[P]$$

and thus $k_{a_1}S_0$ is the steady state flux through the pathway. The concentration of the final product $[P]$ is proportional to $k_{a_1}S_0$.

We then formulate the pathway investment minimization problem as the strategy of minimizing the amount of anabolic substrate for a given flux:

$$\min_{\{[E_i],[S_i],i=1,\ldots,n\}} C([E_i],[S_i]) \quad \text{subject to } n \text{ constraints} \qquad (1)$$
$$\frac{k_i[E_i][S_i]}{\kappa_i + [S_i]} = k_{a_1}S_0 \text{ for } i = 1, ..., n.$$

The optimization is over substrate S_i and enzyme E_i concentrations. Solving (1) using Lagrange multipliers results in the following system of equations:

$$a_i = \lambda_i \frac{k_i[S_i]}{\kappa_i + [S_i]},\ b_i = \lambda_i \frac{k_i\kappa_i[E_i]}{(\kappa_i + [S_i])^2},\ k_{a_1}S_0 = \frac{k_i[E_i][S_i]}{\kappa_i + [S_i]}.$$

Solving the system of equations gives:

$$[S_i] = \sqrt{k_{a_1}S_0\frac{\kappa_i}{k_i}\frac{a_i}{b_i}},$$

$$[E_i] = \frac{b_i}{a_i\kappa_i}[S_i](\kappa_i + [S_i]) = \sqrt{k_{a_1}S_0\frac{b_i\kappa_i}{k_ia_i}} + \frac{k_{a_1}S_0}{k_i}.$$

Therefore the minimum anabolic investment to achieve a flux $k_{a_1}S_0$ through the enzymatic pathway is:

$$C = \sum_{i=1}^{n}([E_i]a_i + [S_i]b_i) = \sum_{i=1}^{n}\left(\frac{a_i}{k_i}k_{a_1}S_0 + 2\sqrt{\frac{\kappa_i a_i b_i}{k_i}k_{a_1}S_0}\right)$$

The impact of different flux levels on the relative total investment requirement is shown in Figure 1. This figure shows that reducing the flux from a baseline value of 1.0 causes an increase in the relative investment cost, but increasing the flux leads to a decrease in the relative investment cost. The key observation we make is that $C(k_{a_1}S_0)$ is an increasing, concave down function of $k_{a_1}S_0$:

$$\frac{\partial C}{\partial(k_{a_1}S_0)} = \sum_{i=1}^{n}\left[\frac{a_i}{k_i} + \frac{1}{\sqrt{k_{a_1}S_0}}\sqrt{\frac{\kappa_i a_i b_i}{k_i}}\right] > 0,$$

$$\frac{\partial^2 C}{(\partial(k_{a_1}S_0))^2} = -\frac{1}{2}\sum_{i=1}^{n}\left[\frac{1}{\sqrt{(k_{a_1}S_0)^3}}\sqrt{\frac{\kappa_i a_i b_i}{k_i}}\right] < 0.$$

As a consequence, if one compares the carbon investment, C, needed to achieve a flux $k_{a_1}S_0$ to the investment needed to achieve twice the flux, $2k_{a_1}S_0$, this investment is *less* than $2C$ representing an enhanced functional return on a given anabolic resource investment. From an ecological perspective, the complete oxidation of a substrate at a fixed flux in a single population will require more anabolic resource investment (approximately 15% more for the parameter choices in Figure 1) to achieve than in a food chain of two interacting microbial populations that split the same substrate oxidation pathway. This observation assumes efficient metabolite exchange between the two food chain populations.

3 Second Benefit: Inhibitory Byproduct Consumption

All metabolisms have byproducts which can negatively influence chemical thermodynamics as well as stress microorganisms by creating inhibitory local environments. Common metabolic byproducts that can be inhibitory include organic acids and alcohols such as formic acid, acetic acid, ethanol, pyruvic acid, lactic acid or glycerol. An existing individual-based model of microbial growth in a biofilm was modified to compare the growth of a monoculture generalist population to a community of cross feeding populations [14]. Biofilms are aggregates of cells encapsulated within a polymeric matrix of microbial origin. Biofilm communities were studied because product inhibition is especially significant in an environment where metabolite transport is limited to

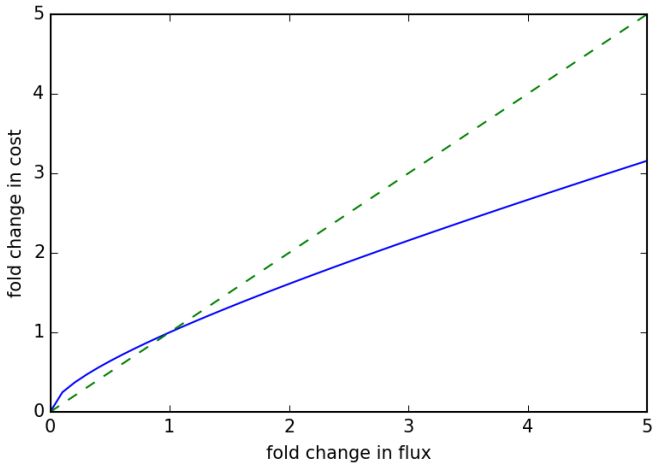

Figure 1: For a fold change in the flux, the fold change in the total anabolic resource investment can be higher for a reduced flux or lower for an increased flux (solid line). The dashed line shows an equal fold change in resource investment for a desired fold change in flux.

diffusion; convective transport is negligible in typical biofilms [12]. Communities of different microbial populations are compared in the simulations. The communities are based on three unique populations:

1. a generalist population that consumes sugar and produces an inhibitory byproduct (e.g., acetate) as well as CO_2,

2. a producer population that consumes sugar and produces only an inhibitory byproduct (e.g., acetate), and

3. a scavenger population that consumes the inhibitory byproduct as its only substrate producing CO_2.

These representative microorganisms and their interactions, which are summarized in Figure 2, are relevant to many natural and engineered systems including the syntrophic consortium studied by Bernstein et al. [3, 4].

Individual-based models, in which individual cells are explicitly modeled and substrate concentrations are modeled using a continuum approximation, are a natural choice for biofilm community simulations. Numerous individual-based models have been developed, and they often focus on different physical aspects of the biofilm environment, from growth to chemical transport to detachment [1, 7, 8]. The individual-based biofilm model analyzed here

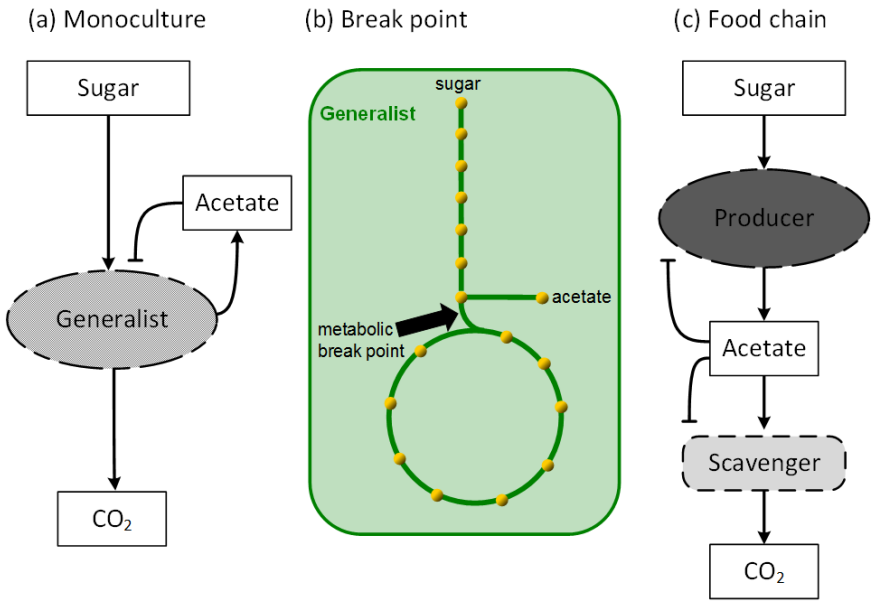

Figure 2: (a) The monoculture contains only the generalist strain, which consumes sugar and produces both an inhibitory byproduct and CO_2. (b) The break point in the metabolic pathway, which can represent a number of commonly observed byproducts, is shown for division of the pathway between the two specialists. (c) The food chain consists of a producer that consumes sugar and produces the inhibitory byproduct, and a scavenger that consumes (and is inhibited by) the byproduct from the producer and secretes CO_2.

is described in two sections: (1) the diffusible substrate model, and (2) the microbial cell model.

3.1 Diffusible Substrate Model

Substrates considered in the biofilm model include a sugar, which serves as the reduced carbon source for the generalist and producer populations, and a reduced metabolic byproduct such as acetate or lactate, that is the carbon and energy source for the scavenger population. Local substrate, S, concentrations within the biofilm are modeled using the reaction-diffusion equation:

$$\frac{dS}{dt} = \mathcal{D}_S \nabla^2 S + \sum_i \left(\frac{1}{Y_{s,i}} \frac{dX_i}{dt} \right) \tag{2}$$

where $\mathcal{D}_S$ is the diffusivity of substrate S within the biofilm , $Y_{s,i}$ is the yield of microbial strain i consuming or producing substrate S, and $\left(\frac{dX_i}{dt}\right)$ is the

specific growth rate of the individual microbial cell i. The diffusivity of sugar is $0.85\ mm^2/h$ assuming a six carbon sugar and the inhibitory byproduct diffusivity is $0.99\ mm^2/h$ assuming a short chain organic acid. The other parameters in equation 2 are dependent on the specific population phenotype, and are defined in the next section. The domain is assumed to have walls (i.e., no-flux boundary conditions) on the bottom and sides, while the top is assumed to have a fixed substrate concentration (1.0 g/L for sugar and 0.0 g/L for inhibitory byproduct). The initial condition is a concentration of zero for all substrates set, in part, to capture the initial slow growth phase when the biofilm is initially being established.

3.2 Microbial Cell Model

While substrates are modeled using a continuum approximation, microorganisms are modeled as discrete cells, which allows each cell to potentially have a unique metabolism. For the presented study, three microbial populations are modeled. The growth rates of the generalist population and the producer population are described by:

$$\frac{dX_i}{dt} = \left(\frac{\mu_i G}{K_{G,i} + G}\right)\left(\frac{K_{I,i}}{K_{I,i} + A}\right) X_i$$

where G is the local sugar concentration (g/L), μ_i is the maximum specific growth rate of population i, $K_{I,i}$ is the byproduct inhibition constant for population i, $K_{G,i}$ is the half-saturation constant for population i, and A is the local byproduct concentration (g/L). The effect of byproduct concentration on specific growth rate of the producer and generalist populations is shown in figure 3a where the byproduct acts as an inhibitor to growth. The specific growth rate of the scavenger population is calculated using:

$$\frac{dX_s}{dt} = \left(\frac{\mu_s A}{K_A + A + \frac{A^2}{K_{IA}}}\right) X_s$$

where K_A is the half-saturation constant and K_{IA} is the byproduct inhibition constant. The effect of byproduct concentration on the growth rate of the scavenger population is shown in Figure 3b where the byproduct is both the sole energy source and inhibitor. The parameter values used in the cell growth equations are summarized in Table 1.

The individual biofilm model algorithm is implemented using the Python programming language and is publicly available on github [15]. The algorithm begins with a setup phase where the initial cell distributions and initial substrate concentrations are set. Then, a time loop is initiated and each time

Param.	Value	Param.	Value	Param.	Value
μ_g	$0.4\ h^{-1}$	μ_p	$0.36\ h^{-1}$	μ_s	$0.4\ h^{-1}$
$K_{G,g}$	$0.05\ g/L$	$K_{G,p}$	$0.05\ g/L$	K_A	$0.005\ g/L$
$K_{I,g}$	$0.04\ g/L$	$K_{I,p}$	$0.15\ g/L$	K_{IA}	$0.5\ g/L$
$Y_{G,g}$	$0.15\ gX/gG$	$Y_{G,p}$	$0.14\ gX/gG$		
$Y_{A,g}$	$0.25\ gX/gA$	$Y_{A,p}$	$0.22\ gX/gA$	$Y_{A,s}$	$0.3\ gX/gA$

Table 1: Parameters used in the individual-based biofilm model and where g is the generalist population, p is the producer population, and s is the scavenger population. See [5] and references therein for source information.

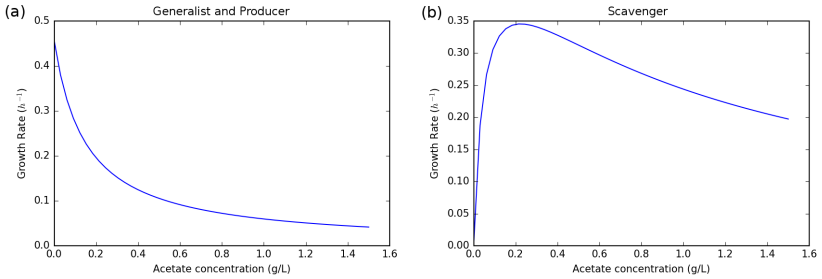

Figure 3: (a) The effects of byproduct inhibition on the specific growth rate of the generalist and producer populations at a fixed sugar concentration of $1\ g/L$, and (b) the effects of byproduct concentration on the scavenger population where the byproduct of the producer population is both the sole energy source and an inhibitor.

step begins with a calculation of the growth of each cell based on the current substrate concentration at the individual cell location. The mass of each cell is increased based on the growth rate and time step. Next, the reaction-diffusion equation is solved to determine updated substrate concentrations. Finally, any cells that have increased in mass beyond a threshold (twice their initial mass for the results shown here) are divided into two cells with one occupying the original location and the other being randomly placed within a cell diameter of the parent microorganism. If any cells are overlapping, i.e., occupying the same space, an iterative smoothing process is used to spread out the cells until no overlap exists.

3.3 Individual-Based Biofilm Model Results

The impact of resource partitioning is illustrated via comparison of three different microbial communities. Initial conditions consisted of 36 cells for all communities; when interacting communities were analyzed the 36 cells were

System	g count	p count	s count	total count
1	389	0	0	389
2	0	288	147	435
3	165	192	109	466

Table 2: Cell counts after simulating 10 hours of growth for an initial community of 36 cells (evenly divided among the relevant three populations). g is the generalist population, p is the producer population, and s is the scavenger population. The values represent the average from 8 independent simulations.

divided equally between population types, e.g. for the two population communities there were initially 18 cells from each population. The first, and simplest community consisted of only the generalist population. The second community consisted of the producer and scavenger populations, and the third community combined generalist, producer, and scavenger populations.

Table 2 summarizes the final population cell counts after simulating 10 hours of growth for all three communities. In all cases, the initial community was comprised of 36 total cells that were randomly placed within two cell diameters of the bottom of the domain. The presented population cell counts are averages of 8 different simulations. The standard deviation of the 8 simulations based on different random starting locations was 5-10 cell counts. It is also important to emphasize that in the mathematical model, starting location is the only source of randomness.

Figure 4a shows a representative cell distribution for a monoculture community of generalists (green). The cells are drawn larger than their actual size to facilitate visualization. Cell clustering was a result of random, initial cell seeding. Figure 4a also shows contours of the byproduct concentration, an inhibitor for this population. The highest byproduct concentrations are found in the center of large cell clusters and inhibit cell growth. This is the least productive community, having the smallest final cell count.

The second community consisted of producer and scavenger populations. The initial community consisted of 18 cells from each population, and an example of a final cell distribution is shown in figure 4b. The producer population(shown as blue) generated more inhibitory byproduct than the generalist population; however, the highest byproduct concentrations were comparable to the generalist monoculture due to the function of the scavenger population (red). The scavenger population grew fastest in regions of high byproduct concentration. The average byproduct concentration in this community was lower than the generalist monoculture, and the overall biomass productivity (i.e., final total cell count) of the community was significantly (10%) higher.

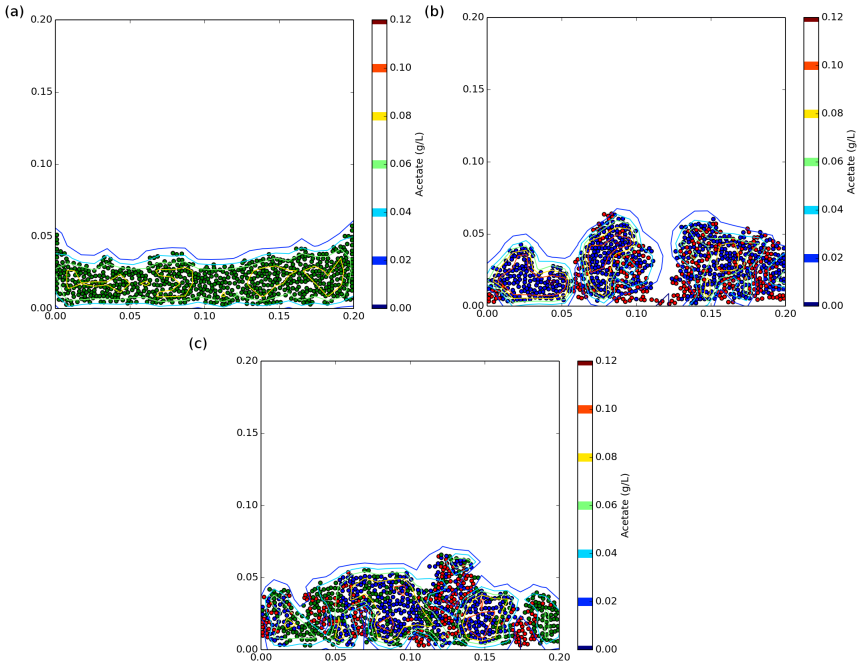

Figure 4: Examples of final microorganism populations after 13 hours of growth for: (a) a monoculture community comprised of the generalist population (green circles), (b) a food-chain community consisting of producer (blue) and scavenger (red) populations, and (c)a diverse community consisting of all three populations: generalist (green), producer (blue), and scavenger (red).

The third community was a combination of the first two communities, and consisted of all three populations considered here: (1) generalist, (2) producer, and (3) scavenger. The initial community was 12 cells of each population for a total of 36 cells. As shown in table 2, this combined community had the largest biomass productivity. An example of a final cell distribution is shown in figure 4c. In some cases, this community had the highest byproduct concentration due to the larger populations of generalist and producer. However, the average concentration never rose significantly higher than the other two communities due to byproduct consumption by the scavenger population.

4 Conclusions

Microbial food chains can represent an ecologically competitive partitioning of environmental resources. Resource partitioning via crossfeeding can potentially benefit a community in numerous ways, and two specific advantages are examined here. First, it was shown through analysis of resource partitioning into substrate and enzyme pools that division of labor via interaction populations can maximize cell function (e.g. flux) for a limiting anabolic resource investment. Second, dividing metabolic processes between cell populations allows the community to avoid a large accumulation of inhibitory byproducts, enhancing overall community productivity. Since different metabolic byproducts present varying degrees of inhibition, resource investment, and energy demand, there is a wide range of benefits from resource sharing in microbial communities. As research and commercial interest in microbial consortia increases, a better quantitative understanding of the benefits of resource sharing will be important for rational engineering and control.

References

[1] Alpkvist, E., C. Picioreanu, M.C.M. van Loosdrecht, and A. Heyden (2006) Three-dimensional biofilm model with individual cells and continuum EPS matrix. *Biotech. Bioeng.*, **95**(5):961-79.

[2] Beck, A., K.A. Hunt, H.C. Bernstein, and R.P. Carlson (2016) Interpreting and designing microbial communities for bioprocess applications, from components to interactions to emergent properties. *Biotechnologies for Biofuel Production and Optimization.* **1**: 407-432.

[3] Bernstein, H.C., S.D. Paulson, and R.P. Carlson (2012) Synthetic Escherichia coli consortia engineered for syntrophy demonstrate enhanced biomass productivity. *J. Biotechnology*, **157**(1):159-66.

[4] Bernstein, H.C. and R.P.Carlson (2014) Design, Construction, and Characterization Methodologies for Synthetic Microbial Consortia. *Methds Mol. Biol.*, **1151**:49-68.

[5] Harvey, E., J. Heys, and T. Gedeon (2014) Quantifying the effects of the division of labor in metabolic pathways. *J. Theor. Biol.*, **360**:222-42.

[6] Holland, J.N. and D.L. DeAngelis (2009) Consumer-resource theory predicts dynamic transitions between outcomes of interspecific interactions. *Ecol. Lett.*, **12**: 1357-66

[7] Kreft, J.U., C. Picioreanu, J.W.T. Wimpenny, and M.C.M. van Loosdrecht, (2001) Individual-based modelling of biofilms. *Microbiology-Sgm.*, **147**:2897-912.

[8] Picioreanu, C., J.U. Kreft, and M.C.M. van Loosdrecht (2004) Particle-based multidimensional multispecies biofilm model. *Appl. Env. Microbiology*, **70**:3024-40.

[9] Rosenzweig, R.F., R.R. Sharp, D.S. Treves, and J. Adams, (1994) Microbial Evolution in a simple unstructured environment: Genetic Differentiation in Escherichia-Coli. *Genetics*, **137**(4):903-17.

[10] Schink, B. (2002) Synergistic interactions in the microbial world. *Anton Leeuw Int. J.*, **81**(1-4):257-61.

[11] Smith, H.L. and P. Waltman, (1995) The theory of the chemostat. *Cambridge University Press*, Cambridge.

[12] Stewart, P.S. and J.B. Raquepas, (1995) Implications of Reaction-Diffusion Theory for the Disinfection of Microbial Biofilms by Reactive Antimicrobial Agents. *Chem. Eng. Sci.*, **50**(19): 3099-104.

[13] Stump, S. M. and C. A. Klausmeier, (2016) Competition and coexistence between a syntrophic consortium and a metabolic generalist, and its effect on productivity. *J Theo Biology* **404**: 348-360.

[14] Venters, M., R.P. Carlson, T. Gedeon, and J.J. Heys, (2017) Effects of Spatial Localization on Microbial Consortia Growth, *PLoS ONE, accepted.*

[15] https://github.com/jeffheys/biofilmSegregation